2-layer Interference Coordination Framework Based on Graph Coloring Algorithm for A Cellular System with Distributed MU-MIMO

Chang Ge, *Student Member, IEEE*, Sijie Xia, *Student Member,IEEE*, Qiang Chen, *Senior Member, IEEE*, Fumiyuki Adachi, *Life Fellow,IEEE*

***Abstract*—In this study, a cellular system with a large-scale distributed multi-user multi-input multi-output (MU-MIMO) is considered, in which a large number of distributed antennas are deployed spatially over each base station coverage area (cell) and user clusters are formed in each cell to perform cluster-wise distributed MU-MIMO in parallel. In such a cellular system, the intercell and intracell interferences coexist and limit the link capacity. In this study, a 2-layer interference coordination (IC) framework that can effectively mitigate the two types of interferences simultaneously is proposed. In the $1^{\rm st}$ layer, the intercell IC is performed in a centralized manner by the non-real-time (non-RT) radio access network intelligent controller (RIC), and then in the $2^{\rm nd}$ layer, under the condition of the results in the $1^{\rm st}$ layer, intracell IC is done by each near-RT RICs in a decentralized manner. Furthermore, a restricted conditional graph coloring algorithm (RCGCA) suitable for this 2-layer IC framework is proposed. The proposed RCGCA is designed to be applied on a partial pre-colored graph, such that when it is applied in the 2-layer IC framework, it satisfies the requirement that the $2^{\rm nd}$ layer coloring must be applied under the condition of the pre-coloring results of the $1^{\rm st}$ layer. In addition, by restricting the total number of colors, the RCGCA can tradeoff between improving the capacity due to interference mitigation and degrading the capacity due to bandwidth partition, thereby maximizing the link capacity. We compare the link capacity achievable by the proposed 2-layer IC framework based on RCGCA with that achievable by the well-known fractional frequency reuse (FFR) scheme, no interference coordination case, fully centralized framework, and fully decentralized framework. Computer simulations confirm that our proposed 2-layer IC framework based on RCGCA can significantly improve the link capacity.**

***Index Terms*—Interference coordination, graph coloring algorithm, distributed MU-MIMO, O-RAN, computational geometry, ultra-dense cellular network.**

I. Introduction

BECAUSE mobile data traffic keeps growing year over year, commercial deployments of 5G have begun in many countries [1]. The rapid increase in the number of users and devices has been leading to the densification of radio access network (RAN) [2] A simple RAN densification approach is to deploy a large number of small-cell base stations (BSs) in the macro-cell area. However, the frequent handoff due to user movement will increase the control signaling traffic, thereby reducing the system capacity to provide data services [3]. Therefore, to alleviate frequent handoff problem, the RAN densification based on massive multi-user multi-input multi-output (MU-MIMO) [4] has been under study.

For massive MU-MIMO, two main approaches exist, namely co-located MU-MIMO and distributed MU-MIMO [5]. For co-located MU-MIMO, an array antenna with a massive number of antenna elements is deployed at the BS, and narrow beams are formed for users in the base station coverage area (cell). While for the distributed MU-MIMO, a massive number of distributed antennas (DAs) each with the radio unit is deployed spatially over the cell, and connected to the BS via optical fronthaul.

When a mm-wave band is used in 5G and beyond, which is unavoidable since the sub-6GHz band is now heavily used [6], distributed MU-MIMO has a unique superiority over co-located MU-MIMO. Distributed MU-MIMO, with a number of DAs spatially deployed over the cell, is able to solve the problem of radio link blockage owing to the nature of rectilinear propagation [7]. Therefore, the distributed MU-MIMO has gained our interest of study.

The drawback of a large-scale massive MU-MIMO, no matter co-located MU-MIMO or distributed MU-MIMO, is the prohibitively high computational complexity required for multi-user signal processing. Our previous study [8] showed that this computational complexity problem can be mitigated by forming multiple user-centric small-cells called user-clusters (hereafter clusters) . Clusters are formed by grouping the nearby users that cause strong interference to each other and then, a large-scale cell-based MU-MIMO can be divided into several small-scale cluster-based MU-MIMOs in parallel, thereby reducing the computational complexity.

However, the introduction of clusters brings a new kind of interference to the system, known as the inter-cluster interference. The inter-cluster interference can be of two types: intracell interference and intercell interference [9]. The intracell interference is caused between clusters which belong to the same cell, while the intercell interference is caused between clusters which belong to different cells and face each other along a cell boundary. The intracell and intercell interference are coupled with each other, and make the interference coordination (IC) faced by cluster-wise distributed MU-MIMO very complicated.

A part of this work was conducted under "R&D for further advancement of the 5th generation mobile communication system" (JPJ000254) commissioned by Research and Development for Expansion of Radio Wave Resources of the Ministry of Internal Affairs and Communications in Japan. (Corresponding author: Chang Ge).

C. Ge, S. Xia, Q. Chen are with the School of Engineering, Tohoku University, Sendai, 980-8579, Japan (e-mail: ge.chang.q2@dc.tohoku.ac.jp; xia.sijie.p2@dc.tohoku.ac.jp; qiang.chen.a5@tohoku.ac.jp;). F. Adachi is with International Research Institute of Disaster Science, Tohoku University, Sendai, 980-8572 Japan (e-mail: fumiyuki.adachi.b4@tohoku.ac.jp).

The intercell and intracell ICs should be treated with different perspectives. The intracell interference is caused by clusters belonging to the same cell. The movement of users results in frequent changes in cluster topology. Therefore, the intracell IC is better to be performed by each BS independently in a centralized manner, so as to satisfy the requirements of dynamic and self-adaptive. On the other hand, the intercell interference is caused by clusters belonging to different cells. It is produced when clusters that are located near cell boundaries share the same frequency band. Considering the system scalability and the limitations of computational complexity in practical, the intercell IC is best performed in a decentralized manner that does not require tight information sharing among BSs.

In co-located MIMO with array antennas deployed, there are many successful IC applications [10][11], but the application of IC in cluster-wise distributed MU-MIMO is still in preliminary stage. In recent years, there are some successful attempts of applying graph coloring algorithm (GCA) to IC. In a small-cell network, H. Zhang, et al. [12] and L. Chen, et al. [13] applied GCA to mitigate co-tier interference. D. Qu, et al. [14] applied GCA to control the intercell interference so as to enhance the spectrum efficiency and user experience for an ultra-dense cellular network. Additionally, J. Mu, et al. [15] applied GCA to solve for IC in fast-changing wireless body area networks (WBANs) of the topology to enhance frequency resource utilization and system stability. In [16], B. Wang, et al. applied GCA to realize co-channel interference management in unmanned aerial vehicle (UAV)-assisted disaster relief networks.

GCA is an algorithm that can assign different colors to neighboring vertices. The GCA-based IC can be regarded as a frequency-domain scheduling. When applying GCA-based IC, the available bandwidth is divided into several sub-bands, each of which represents a corresponding color. Thus, applying GCA ensures that different sub-bands are assigned to neighboring clusters, which as a result, mitigating the interference. However, using GCA pre-supposes the construction of a graph, and to construct a graph, the information must be gathered in a centralized manner. Considering the different perspectives of intercell and intracell IC, the GCA can be used by each BS in parallel as intracell IC.

The application of GCA in each cell independently as intracell IC can effectively mitigate the interference among clusters in the same cell. However, because the coloring results will not be shared among the BSs, the problem of color collision may happen among the clusters which belong to different cells near the cell boundary area, therefore, the intercell interference remains. This leads us to another radio resource allocation-based IC, namely the fractional frequency reuse (FFR) scheme [17]. In cellular systems, the FFR and its variations, such as soft frequency reuse (SFR) [18] and adaptive soft frequency reuse (ASFR) [19], are well-known intercell ICs. The key idea of FFR is to divide users in each cell into two groups, known as inner-cell users and cell-edge users. A frequency reuse factor of n is then applied to cell-edge users, while a reuse factor of one is applied to the inner-cell users. In this way, a different frequency band is allocated to cell-edge users of a different neighboring cell. Therefore, the FFR scheme can realize the intercell IC. However, it should be noted that the use of a reuse factor of n reduces the transmission bandwidth to one part in n accordingly. Therefore, the application of FFR needs to be carefully considered.

Until now, there have been many reports on the successful application of FFR. For example, L. Yang, et al. [20] applied FFR-based IC to enhance the coverage and capacity of a wireless heterogeneous network (HetNet). Furthermore, L. Eslami, et al. [21] proposed a new FFR architecture for IC in a single-cell HetNet containing macro cellular users, D2D users and femto-cell users. A.D. Firouzabadi, et al. [22] demonstrated that FFR techniques significantly improve downlink coverage probability in hybrid full/half duplex (FD/HD) small cell networks. To mitigate the additional intercell interference due to the flexibility of traffic configuration, M. Song, et al. [23] proposed an FFR-based IC for dynamic time-division duplex (D-TDD) small cell networks. In addition, M.Nafees, et al. [24] adopted the FFR scheme in UAV networks to improve the signal-to-interference plus noise ratio (SINR) level of cell-edge users.

In [25], X. Li, et al. proposed an FFR scheme for multi-cell full-dimension MIMO (FD-MIMO) systems, and confirmed that the FFR-based IC scheme can significantly improve the cell-edge performance while maintaining a relatively high total throughput. In [26], T. Saito, et al. applied the FFR scheme to distributed MU-MIMO to enhance the capacity of cell-edge users.

Although it is difficult to directly apply the above mentioned FFR schemes to our system with cluster-wise distributed MU-MIMO, inspired by its core idea, we try to integrate the idea of cell-edge classification from FFR into GCA, thereby taking intercell IC into consideration while ensuring the effect of intracell IC. In this study, we try to realize intercell and intracell IC simultaneously by classifying clusters into cell-edge clusters and inner-cell clusters, and providing them with different available color options during the coloring process. To realize a reasonable allocation of available color options to the cell-edge clusters and the inner-cell clusters, a novel IC framework that provides hierarchical support for GCA is also essential.

Based on the discussions above, we summarize the contributions of this study as follows:

1) Firstly, based on the Open RAN (O-RAN) architecture [27], we propose a 2-layer IC framework that can consider intercell and intracell interferences simultaneously for a cellular system with cluster-wise distributed MU-MIMO. The 1^{st} layer IC is performed by non-real-time (non-RT) RAN Intelligent Controller (RIC) with its broaden perspective on the network to mitigate intercell interference, and the 2^{nd} layer IC, performed by each near-real-time (near-RT) RICs, is to mitigate intracell interference under the conditions of the intercell IC result of the 1^{st} layer.
2) Secondly, with computational geometry (CG), we propose a method to abstract the IC problem as a graph, and successfully solve the threshold optimization problem

during graph construction by constructing Delaunay Triangulation and Minimum Spanning Tree.

3) Thirdly, we propose a restricted conditional GCA (RCGCA) to be applied to the 2-layer IC framework. The proposed RCGCA is based on a partial pre-colored graph. The reason for this is that when the RCGCA is applied to the 2-layer IC framework, the 1st layer's cell-edge coloring results will become a pre-condition for the 2nd layer inner-cell coloring. In addition, the RCGCA is designed to restrict the total number of colors, which enables the RCGCA to tradeoff between improving the capacity due to interference mitigation and degrading the capacity due to bandwidth partition, thereby maximizing the link capacity.

The remainder of the paper is organized as follows. In Section II, we explain our system structure and provide the problem statement. In Sections III and IV, the proposed 2-layer IC framework and RCGCA, respectively, will be described in detail. In Section V, the 2-layer framework will be combined with RCGCA, and the results of performance evaluation using Monte-Carlo simulations is provided in Section VI. Finally, the conclusions will be drawn in Section VII.

Notations: Throughout this paper, we will use the word "color" to indicate a certain sub-band obtained by partitioning the system bandwidth.

II. System Structure and Problem Statement

The proposed 2-layer IC framework is designed to be deployed in O-RAN [27] as shown in Fig.1. The O-RAN, through its disaggregated, hierarchical, adaptive network function processing architecture, aims to build a radio network that is intelligent, multi-vendor, software-driven, flexible and dynamic, so as to fulfill the needs of the next generation mobile networks [28]. The key functional components introduced by O-RAN architecture is the non-RT RIC and the near-RT RIC [29].

The non-RT RIC, with a control loop on the order of seconds or minutes, is responsible for global monitoring and optimization, as well as providing policy-based guidance to support the operation of near-RT RICs. While the near-RT RICs, whose control loop is between 10ms to 1s, is the specific executor, and is responsible to perform tasks such as policy enforcement or radio resource management for one or several cells [30]-[35].

In this study, we considered a cellular system with cluster-wise distributed MU-MIMO, the structure of which is illustrated in Fig. 2. The wide communication service area, which comprises a large number of DAs, is divided into a prescribed number of cells. The non-RT RIC, with its broaden perspective on the network, is used to perform cellular construction based on the location of DAs. The near-RT RIC, which is connected with the O-DU, O-CU-CP/Up via the E2 interface, is responsible for forming user-clusters inside a cell, and cluster-wise MU-MIMO is carried out in parallel. In this study, this communication system is termed as the cellular system with cluster-wise distributed MU-MIMO. In such a cellular system, there are two types of interferences: intercell interference and

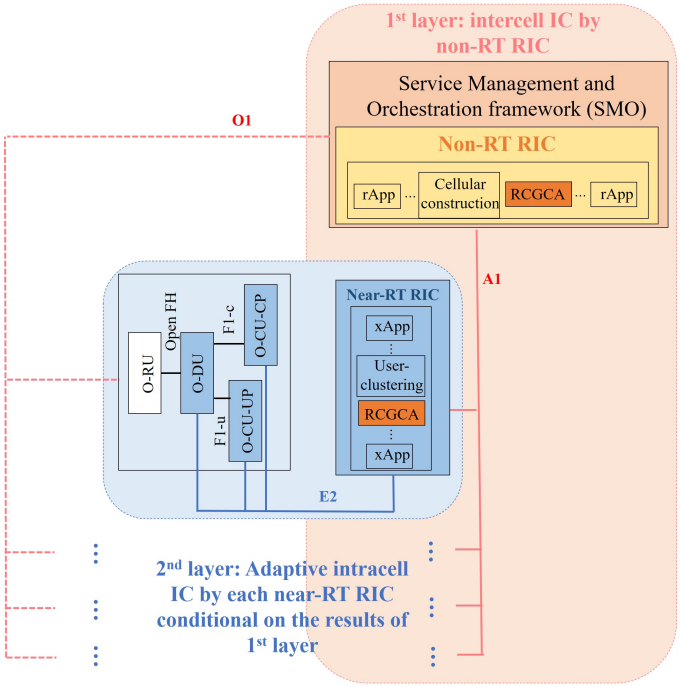

Fig. 1. 2-layer IC framework in O-RAN.

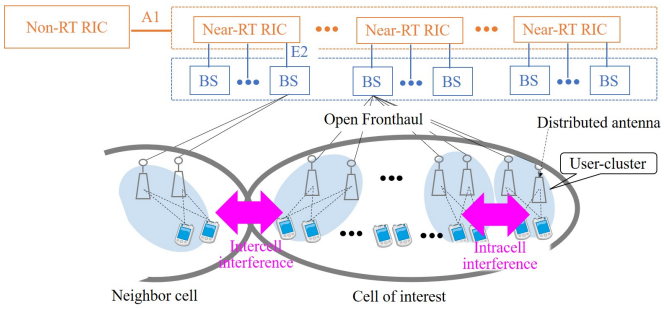

Fig. 2. Structure of a cellular system with distributed MU-MIMO.

intracell interference. Both these interferences are essentially inter-cluster interferences, but because some clusters belong to the same cell and other clusters belong to neighboring cells, the problem of IC becomes very complicated.

Basically, there are two IC frameworks, namely the fully centralized (FC) framework and fully decentralized (FD) framework. In FC framework, after the user-clustering is conducted by each near-RT RICs, the non-RT RIC collects the information of all the clusters via A1 interface, and then, is responsible for conducting IC for all clusters inside the entire service area. Because the FC framework can coordinate both intercell and intracell interferences at the same time, it can achieve better IC performance. However, it is also obvious that the FC framework has a very high computational complexity. Meanwhile, for the users with high mobility, it is difficult for the non-RT RIC to realize the dynamic control. Therefore, the results of FC framework can only be regarded as an ideal benchmark, and is difficult to be utilized in practical applications.

Another practical alternative is the FD framework. In FD framework, each near-RT RIC conducts intracell IC indepen-

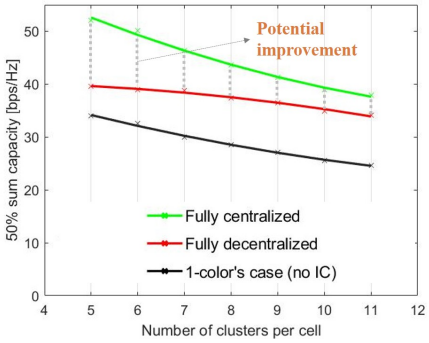

Fig. 3. 50% sum capacity comparison of FC and FD frameworks.

dently, and the non-RT RIC does not need to participate. The FD framework distributes the computational load from the non-RT RIC to each near-RT RICs, however, because the cells are considered isolated from each other, the intercell interference cannot be taken into account, and thus it remains. Therefore, the FD framework cannot achieve a similar good interference mitigation as the FC framework, and accordingly, the link capacity obtained by the FC framework is higher than that by the FD framework.

In Fig. 3, the 50% sum capacities (the sum capacity at a cumulative distribution function (CDF) of 50%) achievable by the FC and FD frameworks are plotted as a function of the number of clusters (note that the detailed simulation setting is explained in Section VI). In this study, we attempt to solve the contradiction between FC and FD framework by proposing a novel 2-layer IC framework. The proposed 2-layer IC framework allows the two kinds of RICs to cooperate with each other and fully exploit their respective advantages, thus is able to fill the performance gap between the FC and FD frameworks while maintaining the computational complexity at a low level. It can be considered that our proposed 2-layer IC framework is a new attempt in O-RAN for IC based on the coordination of RICs.

III. Proposed 2-layer Interference Coordination Framework

Our proposed 2-layer IC framework is illustrated in Fig. 1 and Fig. 2. In the 1st layer of IC, the location information of DAs is gathered by the O1 interface to the non-RT RIC, and the so-called non-RT RIC applications (rApps) are responsible for constructing cells based on the location of DAs, and coordinating the intercell interference with the help of cell centroid information. The results of intercell IC will be passed via A1 interface to the near-RT RICs. Because the DAs' locations are stable in general, the 1st layer IC is only carried out when cellular reconfiguration is updated, therefore this kind of large-timescale operation task fits well with the control loop of non-RT RIC.

In the 2nd layer of IC, each near-RT RIC, which is connected with the O-CU-CP/UP and O-DU via the high-speed E2 interface, is responsible to obtain the information of users' location. Then the near-RT RIC applications (xApps) are responsible for forming clusters and coordinating the intracell interference under the conditions of the result of the 1st layer IC. Implementing the 2nd layer of IC on the xApp of near-RT RIC, rather than locally at the BS, takes full advantage of the O-RAN architecture and meets the purpose of introducing RICs and the A1 interface. Also, the advantages of applying xApp of near-RT RIC over local control of BS is that it makes the introduction of artificial intelligence possible in the future.

The 2-layer IC framework can be classified as a semi-decentralized framework that adds an additional centralized layer on top of the decentralized layer. Compared with the FC framework, the 2-layer IC framework is feasible in practical because the non-RT RIC only needs to coordinate the relationship among cells rather than coordinating all the clusters, and the task of coordinating the clusters is delegated to each corresponding near-RT RICs. Compared with the FD framework, the 2-layer IC framework is able to consider intercell interference without information sharing among the BSs. In this study, we also propose a RCGCA to be applied to the 2-layer IC framework, as both the rApp in non-RT RIC and xApp in near-RT RICs. and the details will be explained in the next section.

The "openness" of O-RAN enables substantial flexibility of its deployment, and each near-RT RIC can be flexibly configured with one or several BSs [36]. Our proposed 2-layer IC framework works the same way regardless of the number of BSs. For the sake of simplicity and without loss of generality, in the following sections of this paper, in order to enable easy illustration of how our proposed 2-layer IC framework works based on RCGCA, we assume each near-RT RIC controls one cell independently.

IV. Proposed Graph Coloring Algorithm

In this section, we propose a RCGCA that is designed for the 2-layer IC framework. The graph coloring problem is derived from graph theory. First, we need to abstract the IC problem as a graph; hence, in subsection A, we will introduce how the graph is constructed using CG. The details of our proposed RCGCA, including how to introduce the restriction and conditions into the original heuristic GCA, are then explained in subsection B.

A. Graph construction

The interference in a wireless communication system is bidirectional; therefore, it can be simplified as an undirected graph $G = (V, E)$, where V and E denote the set of vertices and edges, respectively. With G, our IC problem can be abstracted as a vertex coloring problem, which refers to coloring the vertices so that any two vertices with connected edges do not share the same color.

In this study, it is assumed that the non-RT RIC form cells and each near-RT RICs form user-clusters based on the K-means algorithm [37]. Each cell and cluster can be represented by their corresponding centroids in geometric position. Therefore, V denotes the centroids of clusters or cells. E denotes the mutual adjacency relationship among the vertices, as the most severe interference exists between neighboring vertices.

V is easily obtained because once the non-RT RIC and each near-RT RICs apply the K-means algorithm as rAPP or xApp, the location information of the centroids is known; however, E cannot be obtained directly. To define E, we need to derive the relative adjacency relationship from the position information of the centroids.

A commonly used method is to use the threshold [12]–[14]. However, the optimum threshold value is usually obtained via optimization algorithm, which is not applicable in the case of dynamically changing user locations and cluster topology. Therefore, in this study, we propose to apply the Delaunay Triangulation [38] from CG to help decide the adjacency relationship and thus circumvent the threshold optimization problem. The Delaunay Triangulation is a classic triangulation method with linearithmic time complexity. For the given three vertices in V, if the circle circumscribing them does not contain any other vertex, the Delaunay Triangulation is satisfied and the result of such triangulation is denoted as DT(V). We apply Delaunay Triangulation on the centroids. If there is a triangle edge connecting two vertices, these two vertices are regarded as neighbors. In this way, the adjacency relationship, or E of graph, can be determined without using the threshold.

The reason why DT(V) can be used to define the adjacency relationship is explained below. There are several characteristics of DT(V), among which the most important one is that it can maximize the minimum angle and avoid sliver triangles (triangles with extremely acute angles) [38]. This characteristic enables allocating the same color to more distant vertices, and therefore, fits well in IC. We take vertices 1–4 in Fig. 4 for illustrating this point. In Fig. 4(d), we provide two triangulation results for the vertices 1–4. DT(V), which is the left one, defines the vertices 1 and 3 as neighbors, while non-DT(V) defines 2 and 4 as neighbors. Thus, using DT(V) can assign the same color to more distant vertices. The interference becomes weaker on average if the pathloss is higher. Because the pathloss is proportional to $d^{-\alpha}$, where d is the distance between the transmitter and receiver, and α is the pathloss exponent, the more distant vertices usually have weak interference with each other.

Furthermore, other characteristics of DT(V) are also worth mentioning. Firstly, the nearest neighbor graph (NNG) has been demonstrated to be a subgraph of DT(V) [38], and because the nearest neighbors usually provide the strongest interference, it can be ensured that the strongest interference will be mitigated. Another characteristic of DT(V) is that the change of any one vertex will only affect its nearby triangles, while the far located vertex's triangulation results remain unchanged. Because of this characteristic, adding or removing several vertices has no effect on the far away vertices, thereby maintaining the system scalability [38].

Because of the structural advantage of triangles, the graph constructed by DT(V) can cope well with the case when M, the restricted maximum number of colors, is greater than or equal to three. However, during the application of RCGCA, M may be set to any value. When $M = 2$, we need to extend further on the basis of the adjacency relationship determined by DT(V) to construct the bipartite graph.

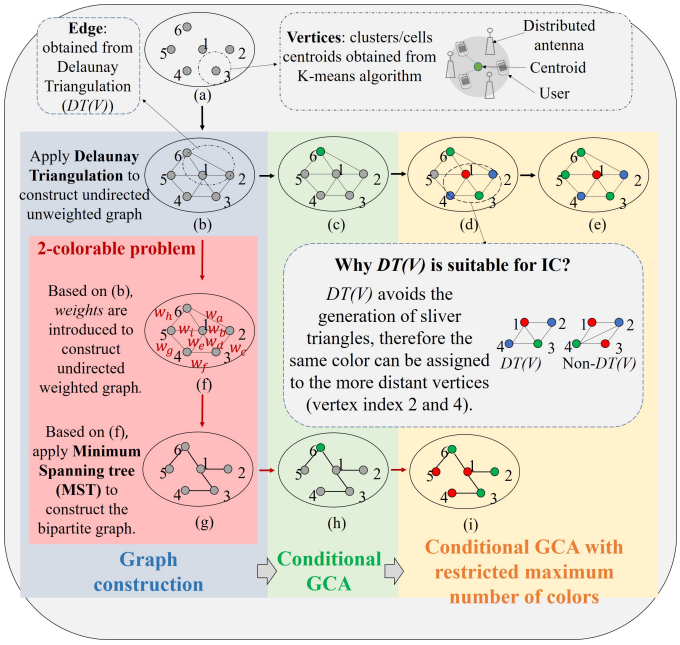

Fig. 4. Graph construction and proposed RCGCA.

In the graph coloring problem, $M = 2$ is known as the 2-colorable problem, and the bipartite graph is proven to be 2-colorable [39]. Based on the undirected unweighted graph G, we introduce weights and further construct the undirected weighted graph $G' = (V', E', W')$, where V', E', and W' denote the set of vertices, edges, and weights, respectively. The weights are determined based on the distance between the centroids in this study.

Based on graph G', minimum spanning tree (MST) [38] is applied to construct the bipartite graph. MST is a spanning tree with minimum sum of weights. Because the weights are defined as distance and the pathloss is inversely proportional to distance, MST connects the paths where the vertices interfere the most with each other. The upgrade of graph construction is illustrated in Fig. 4(f) and Fig. 5(g). The case of $M = 2$ is necessary and its effectiveness will be explained in Section VI, where it will be used in the 1^{st} layer of IC.

MST is a subgraph of DT(V), and the Prim's algorithm or Kruskal's algorithm [40] can be used as faster approaches to solve MST on the basis of DT(V). The application of MST has been considered mainly in adhoc networks to improve the connectivity while solving the tradeoff of power conservation [41]–[43]. It should be noted that to the best of the authors' knowledge, this is the first time to apply MST to solve graph coloring-based ICs. In adhoc networks, MST is used to determine the strongest link of connection. Whereas, in our case, MST is used to determine the strongest link of interference between vertices, and interference mitigation is achieved by breaking these links when different colors are offered.

In our proposed 2-layer IC framework based on RCGCA, the clusters will be classified into cell-edge clusters and inner-cell clusters, and then, colored separately. For the cell-edge classification method, we propose to construct a convex hull [38]. The convex hull, which is also a subgraph of DT(V)

[44], has been used in scenarios such as boundary detection in wireless sensor networks [45]. The application of convex hull enables the determination of clusters located near the cell boundary and classify them as cell-edge clusters.

According to our previous study [46], using CG-based graph construction can achieve the same good result in defining E as using the optimized threshold. Therefore, in the case of dynamically changing user locations and cluster topology, using our proposed method is considered more feasible compared to using the threshold method. Based on the results of DT(V) and MST, the adjacency matrix $\mathbf{A} = (a_{ij}) \in \mathbb{R}^{N\times N}$ can be defined as in (1). The adjacency matrix records the information of V and E in graph, and is the basis of RCGCA.

$$a_{ij} = \begin{cases} 1, & \text{vertex } i \text{ and } j \text{ are connected by DT}(V) \\ 0, & \text{vertex } i \text{ and } j \text{ are not connected by DT}(V) \end{cases} \quad (1)$$

B. Details of proposed RCGCA

After the graph is constructed, the GCA is carried out. The graph coloring problem is a classical combinatorial optimization problem, which usually relies on heuristic algorithms to obtain sub-optimal solutions developed for engineering applications. A few mature heuristic, such as largest degree ordering (LDO), Welsh–Powell, and DSATUR [47] have been proved to be effective in obtaining high quality solutions. In this subsection, we use DSATUR to explain how to add restriction and conditions to heuristic GCA so that it can be applied to our proposed 2-layer IC framework.

The idea of restriction and conditions are illustrated in Fig. 4. To adapt to the 2-layer IC framework, the 2^{nd} layer graph coloring needs to be done under the condition that a few of the vertices have already been colored by the 1^{st} layer coloring process. Therefore, the condition of partial pre-coloring must be added to the traditional heuristic GCA. In Fig. 4(c) and (h), vertex 6 has been colored in advance. GCA that needs to be done for a partial pre-colored graph is named as a conditional GCA in this study. In addition to the condition of partial pre-coloring, in Fig. 4(d), we set a restriction to the total number of colors M available in the coloring process. The use of the restricted maximum number of colors decreases the degree of freedom for vertices; therefore, when $M = 3$ as shown in Fig. 4(d), vertex 5 cannot be colored successfully, or in other words, color collision is unavoidable around vertex 5. Hence, when the restricted maximum number of colors is added to GCA, we must solve the problem of minimizing interference while assuming that color collision cannot be completely avoided (as shown in Fig. 4(e)).

Adding the color number restriction will lead to color collision and the existence of color collision will inevitably cause strong interference. An interesting question is why such a restriction is introduced in the GCA. To explain this, we need to start with the following definitions and theorems.

Definition 1: The chromatic number $\chi(G)$ represents the minimum number of colors required for graph G. In this study, it represents the number of narrow sub-bands into which the system bandwidth is divided.

Definition 2: The degree δ_n of a vertex n represents the number of edges that are incident to the vertex. In this study, it represents the number of neighbors of vertex n.

Theorem: For a graph G with maximum degree δ_{max}, Brooks' theorem [48] states that at most δ_{max} colors are needed, unless G is a complete graph or an odd cycle. Also, if a heuristic algorithm is applied, $\chi(G)$ is no more than $\delta_{max}+1$ [49].

For a given graph, the traditional vertex coloring problem considers the use of as few colors as possible to complete the coloring while satisfying the requirement that neighboring vertices do not use the same color [50]. In other words, the traditional GCA aims to reduce $\chi(G)$; however, for an arbitrary graph, it cannot guarantee that $\chi(G)$ is less than a certain value. In the cellular system with distributed MU-MIMO considered in this study, the random movement of users brings great uncertainty to the cluster topology, leading to a graph with large δ_{max} sometimes. According to the above theorem, a large δ_{max} can result in large $\chi(G)$ when heuristic GCA is applied. However, when IC is conducted, large $\chi(G)$ means that the system bandwidth must be divided into many narrow sub-bands. Although the interference can be mitigated thoroughly, the link capacity may not be necessarily improved. Therefore, we allow a certain amount of color collision by introducing restrictions into the GCA.

The proposed RCGCA is shown in Algorithm 1. We assume that all vertices that are allocated the same color belong to one color group. Representing the total number of vertices by N, κ_m denotes a set of vertices in the m^{th} color group, $m \in \{1, 2, \ldots, M\}$, where M is the restricted maximum number of colors. The prior coloring result obtained after the 1^{st} layer IC is expressed by the vector $\mathbf{c} = [c_1 \cdots c_N]$ with $c_i \in \{0, 1, 2, \cdots, M\}$ where $c_i = 0$ indicates that vertex i has not been colored in the 1^{st} layer. The proposed RCGCA is modified based on DSATUR, and all the vertices are first arranged as $v_1, v_2, \ldots, v_N$ in descending order of degree δ in steps 1–2, then reset based on the degree of saturation $\delta^{'}$ [47] in step 14 after been colored sequentially in steps 3–13.

During the coloring process in steps 3–13, the conditional GCA with restricted number of colors M is first conducted in steps 5–9. For a vertex v_i, the setting of the restriction M clarifies the available color pool, while the prior coloring results $\boldsymbol{c}$ and adjacency matrix $\mathbf{A}$ together decide the pre-colored conditions; that is, they decide which colors have been pre-colored by neighbors and thus cannot be used. The remaining colors with smallest index will then be assigned to v_i.

After performing steps 5–9, a few vertices may remain uncolored. Steps 10–12 are designed to recolor these uncolored vertices. During the recoloring process, color collision with one or more neighbors is inevitable. To minimize the interference among the inevitable color collision, it is better to assign the same color to the vertices with the least interference between them. As mentioned before, the interference becomes weaker on average if the distance is longer, and therefore, the most distant neighbors should be chosen. Assuming that the location information of cell centroids and that of cluster centroids is known to non-RT RIC and each near-RT RICs, respectively, it is better to assign the same color to the most distant neighbors.

To find the most distant neighbors, we define a relative

distance matrix $\widetilde{\mathbf{D}} = (\widetilde{d}_{ij}) \in \mathbb{R}^{N\times N}$), where

$$\tilde{d}_{ij} = \frac{d_{ij}}{\sum_{j=1,j\neq i}^{N} d_{ij}}, i, j = 1 \sim N \tag{2}$$

with d_{ij} denoting the distance from the centroid of cluster j to that of cluster i. Based on $\widetilde{\mathbf{D}}$, the recoloring process (steps 10–12) is performed. The recoloring process allows the existence of color collision, but minimizes its impact on interference by ensuring that the color collision happens only between the most distant neighbors.

Algorithm 1: Restricted conditional graph coloring algorithm (RCGCA)

Input: $\mathbf{A}, \mathbf{D}, \mathbf{c}, M$
Output: $\kappa_m, \forall m \in M$
1: Initialize δ
2: Sort all vertices in decending order of δ, and set the obtained vertex set as $\mathcal{V}$.
3: **for** $v_i = v_1 : v_N$ **do**
4: **while** $c_{v_i} = 0$ **do**
5: **for** $m = 1 : M$ **do**
6: **if** $m \notin \mathbf{c} \odot \mathbf{A}^{(v_i,:)}$ **then**
7: $c_{v_i} \leftarrow m$
8: **end if**
9: **end for**
10: **if** $c_{v_i} = 0$ **then**
11: $c_{v_i} \leftarrow c_{\arg\max(\tilde{\mathbf{D}} \odot \mathbf{A}^{(v_i,:)})}$
12: **end if**
13: **end while**
14: Reset the vertex set $\mathcal{V}$ based on the degree of Saturation δ'.
15: $\kappa_{c_{v_i}} = \kappa_{c_{v_i}} \bigcup v_i$ % Assigning the vertex to color group.
16: **end for**
(Note that $\odot$ denotes the Hadamard product; $\mathbf{X}^{(y,:)}$ indicates the y^{th} row vectors of the matrix $\mathbf{X}$.)

V. Application of RCGCA to 2-layer IC Framework

In this section, we explain the application of our proposed RCGCA to the 2-layer IC framework. The 2-layer IC framework based on RCGCA is illustrated in Fig. 5. The RCGCA is first applied to the 1st layer as rApp, and then, to the 2nd layer as xApp. In the 1st layer IC, the available frequency band will be divided into several sub-bands (named as total color pool), and the motivation of 1st layer IC is to specify the sub-color pool that can be used by cell-edge clusters of each cell. We assume that the number of total color pool is N_{color}^{total}. Additionally, we assume that the total color pool is divided into N_{sub} sub-color pools, and each sub-color pool has the same number N_{color}^{sub} of colors. Therefore, $N_{color}^{total} = N_{color}^{sub} \times N_{sub}$.

In the 1st layer of intercell IC, the non-RT RIC applies RCGCA-based rAPP for global intercell IC by assigning one of the sub-color pools to each cell. The results of the sub-color pool assignment are passed to the corresponding near-RT RICs as a guidance information to support the operation of near-RT RICs in the 2nd layer IC. Thus, when applying RCGCA-based rAPP in the 1st layer IC, M is set to N_{sub}. Because the cell structure is stable in general if the cellular reconfiguration is not considered, the 1st layer IC is carried out only once.

In the 2nd layer of intracell IC, each near-RT RICs, as the specific IC executors, perform intracell IC independently under the conditions of the results of intercell IC in 1st layer. Firstly, the cell-edge clusters are colored with the sub-color pool assigned in the 1st layer to mitigate the intercell interference. Because the cell-edge clusters are distributed linearly alongside the cell boundary, the intracell interference between cell-edge clusters can be eliminated by arranging N_{color}^{sub} colors sequentially. Then, by setting M to N_{color}^{total}, the remaining inner-cell clusters are colored by RCGCA-based xAPP using the total color pool for mitigating the intracell interference under the condition that the cell-edge clusters have already been colored.

VI. Monte Carlo Simulation

In this section, we will demonstrate the performance evaluation of our proposed 2-layer IC framework based on RCGCA. First, we will describe the construction of a cellular structure. We will then discuss about the optimized parameter setting (N_{sub} and N_{color}^{sub}) for applying RCGCA to the 2-layer IC framework. Using the optimized parameter setting, we perform computer simulations to obtain the link capacity. We then compare our proposed 2-layer IC framework based on RCGCA with the dynamic FFR, no IC case, FC framework, and FD framework to verify the improvement in link capacity.

A. Generation of cellular structure

We consider a normalized area of 5 × 5 over which 3,200 DAs are randomly located and a cellular structure of 25 cells is constructed. First, K-means algorithm is applied to obtain the cell centroids using the location information of DAs. Based on the cell centroids, the cellular structure is constructed by using the centroidal Voronoi tessellations (CVT) [51]. An example of cellular structure is shown in Fig. 6. To accurately estimate the link capacity under the intercell interference environment, the centermost cell is chosen as the cell of interest.

Inside each cell, user-clusters are formed by K-means algorithm. The clustering result is also shown in Fig. 6, where the users in the same cluster are connected to the cluster centroid by solid lines. The serving DAs are then assigned to each user-cluster based on the principle of proximity for conducting cluster-wise distributed MU-MIMO. The DA assignment results are shown as dashed lines in Fig. 6. Finally, because ZF precoding [52] is going to be applied, the number of DAs in each cluster must not be less than the number of users, and the assignment of DAs is further optimized based on our previously proposed trading algorithm [53].

B. Link capacity formula

In this section, we evaluate the downlink sum capacity and user capacity to confirm the performance of our proposed 2-layer IC framework based on RCGCA. As described in Section

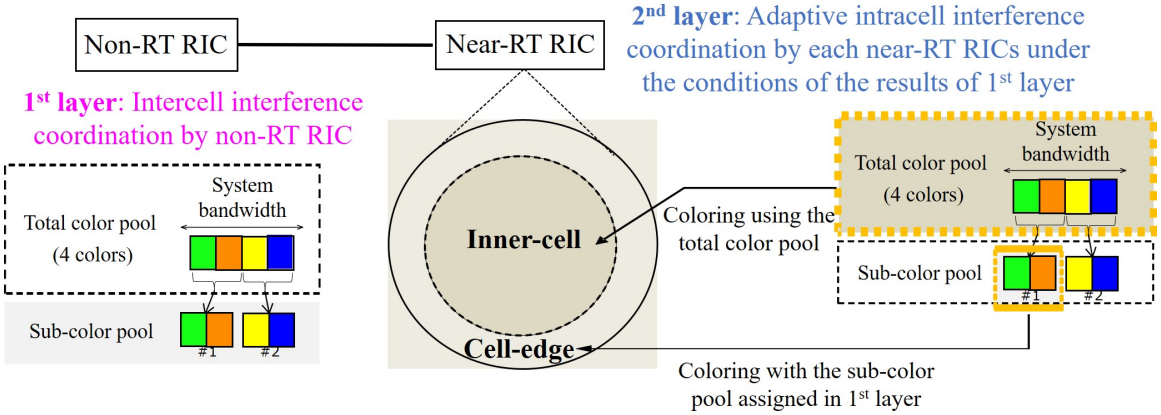

Fig. 5. 2-layer IC framework based on RCGCA.

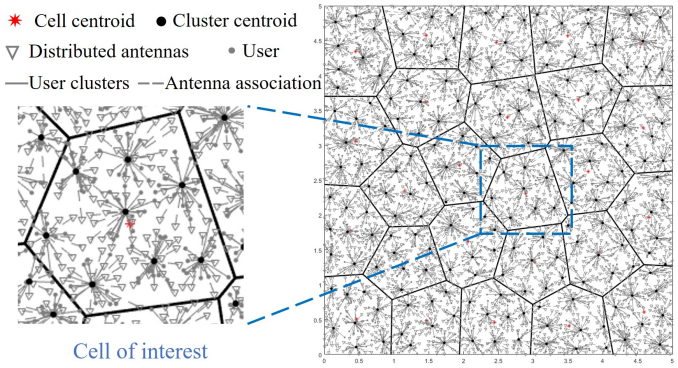

Fig. 6. An example of cellular structure with user-clusters in each cell.

V, after applying 2-layer IC based on RCGCA, each cluster is assigned one color from the total color pool of N_{color}^{total} colors, and all clusters that are assigned the same color belong to one color group. Because a different color corresponds to a different frequency sub-band, the interference exists only inside the color group. Assuming that the number of clusters in each cell is N_C^{cell}, and each cell has the same number of clusters, the total number of clusters in the service area can be obtained as $N_C^{total} = N_C^{cell} \times N_{cell}$. Similarly, the total number of users and DAs in the service area can be denoted as N_U^{total} and N_A^{total}, respectively. In the m^{th} color group, $m \in \{1, 2, \cdots, N_{color}^{total}\}$, the numbers of clusters, users, and DAs are denoted by N_C, N_U, and N_A, respectively. Furthermore, the i^{th} user and j^{th} DA in the k^{th} cluster are denoted by U_i^k and A_j^k , respectively. N_{U^k} and N_{A^k} are the number of users and DAs in the k^{th} cluster, respectively.

In a cellular system with cluster-wise distributed MU-MIMO, the received signal is the superposition of the desired signal, interference, and noise. The interference comprises multi-user interference within each cluster and inter-cluster interference from other clusters (irrespective of being in the same cell or in neighbor cells) that are assigned the same color. Because ZF precoding is used for cluster-wise MU-MIMO, only the inter-cluster interference is considered in this study.

The downlink received signal of user U_i^k can be expressed as

$$y_{U_i^k} = \mathbf{H}_k^{(i,:)} \mathbf{W}_k^{(:,i)} \sqrt{P_k} x_{U_i^k} + \sum_{l=1, l\neq k}^{N_C} \sum_{j=1}^{N_{U^l}} \mathbf{H}_{k,l}^{(j,:)} \mathbf{W}_l^{(:,j)} \sqrt{P_l} x_{U_j^l} + n_{U_i^k} \tag{3}$$

where the first, second, and third terms are the desired signal, inter-cluster interference, and noise, respectively. Note that the matrices are represented as bold upper case letters and the superscripts $(i,:)$ and $(:,i)$ represent the i^{th} row and column vectors of the matrix, respectively.

In (3), $x_{U_i^k}$ and $n_{U_i^k}$ are the transmit signal and noise, respectively. P_k and P_l are the power allocated to the k^{th} and l^{th} clusters, respectively, and can be expressed as

$$P_{k \text{ or } l} = \frac{N_{U^{k \text{ or } l}} P}{\|\mathbf{W}_{k \text{ or } l}\|_F^2} \tag{4}$$

where $\|\cdot\|_F$ stands for the Frobenius norm. P is the normalized transmit signal power-to-noise ratio equal to all P_U users. P is set to 0 dB, indicating that the received signal-to-noise ratio becomes 0 dB when the distance between the transmitter and receiver is equal to unit length in the normalized area of 5 $\times$ 5. Furthermore, $\mathbf{W}_k$ and $\mathbf{W}_l$ are the ZF precoder matrices, which can be expressed as

$$\mathbf{W}_{k \text{ or } l} = (\mathbf{H}_{k \text{ or } l})^\dagger = \mathbf{H}_{k \text{ or } l}^{\mathsf{H}} \left(\mathbf{H}_{k \text{ or } l} \mathbf{H}_{k \text{ or } l}^{\mathsf{H}}\right)^{-1} \tag{5}$$

where $(\cdot)^{\mathrm{H}}$ denotes the conjugate transposition of a matrix.

In (3), $\mathbf{H}_k \in \mathbb{C}^{N_{U^k} \times N_{A^k}}$ is the channel matrix and $\mathbf{H}_{k,l} \in \mathbb{C}^{N_{U^k} \times N_{A^l}}$ is the interference channel matrix between N_{U^k} users of the k^{th} cluster and N_{A^l} DAs of the l^{th} cluster. $\mathbf{H}_k$ and $\mathbf{H}_{k,l}$ can be expressed as

$$\mathbf{H}_k = \begin{pmatrix} h_{11} & \cdots & h_{1N_{A^k}} \\ \vdots & & \vdots \\ h_{N_{U^k}1} & \cdots & h_{N_{U^k}N_{A^k}} \end{pmatrix} \tag{6}$$

$$\mathbf{H}_{k,l} = \begin{pmatrix} h_{11} & \cdots & h_{1N_{A^l}} \\ \vdots & & \vdots \\ h_{N_{U^k}1} & \cdots & h_{N_{U^k}N_{A^l}} \end{pmatrix} \tag{7}$$

In (6) and (7), $h_{a,b}$ is given as

$$h_{a,b} = \sqrt{{d_{a,b}}^{-\alpha}}\sqrt{10^{-\frac{\varphi_{dB}}{10}}}z \tag{8}$$

where $d_{a,b}$ is the distance between the a^{th} user and b^{th} DA, α is the pathloss exponent, φ_{dB} is the shadowing loss, which is characterized by a real-valued zero-mean Gaussian random variable with standard deviation of σ, and z is the Rayleigh fading gain, which is characterized by a complex-valued zero-mean Gaussian random variable with unit variance. In this study, we assume that $\mathbf{H}_k$ and $\mathbf{H}_{k,l}$ are perfectly known.

The received signal-to-interference-plus-noise-ratio ($SINR_{U_i^k}$) of the i^{th} user in the k^{th} cluster is computed by approximating the sum of inter-cluster interference and noise as a complex Gaussian process, and is given as

$$SINR_{U_i^k} = \frac{\left\|\mathbf{H}_k^{(i,:)}\mathbf{W}_k^{(:,i)}\right\|^2 P_k}{\sum_{l=1,l\neq k}^{N_C}\sum_{j=1}^{N_{U^l}}\left\|\mathbf{H}_{k.l}^{(j,:)}\mathbf{W}_l^{(:,j)}\right\|^2 P_l + 1} \tag{9}$$

The $U_i^{k\,\text{th}}$ user capacity $C_{U_i^k}^m$[bps/Hz], m^{th} color group's sum capacity C_{sum}^m[bps/Hz], and system sum capacity C [bps/Hz] are obtained as

$$\begin{cases} C_{U_i^k}^m = \frac{1}{N_{color}^{total}}\log_2\left(1 + SINR_{U_i^k}\right) \\ C_{sum}^m = \sum_{k=1}^{N_C}\sum_{i=1}^{N_{U^k}} C_{u_i^k}^m \\ C = \sum_{m=1}^{N_{color}^{total}} C_{sum}^m \end{cases} \tag{10}$$

C. Simulation results

The parameter setting for computer simulation is shown in Table I. For simulation, a quasi-static environment is considered, implying that user locations remain the same during their communication duration. The quasi-static channel is realized by generating shadowing loss and Rayleigh fading gain for each user location. The user locations are generated randomly for 100 times. For each generation of user locations, the shadowing loss of each user is generated 10 times, and for each generation of shadowing loss, the Rayleigh fading gain for each user is generated 10 times. As a consequence, the total number of channel realizations is 10,000. For each generation of user locations, clustering and 2-layer IC based on RCGCA are carried out and the user capacity, sum capacity per color group, and system sum capacity are then computed using (10) for obtaining their CDF. N_{color}^{total}, N_{sub}, and the corresponding N_{color}^{total} will be determined after optimization, as shown in the following subsection.

1) **Parameter optimization**

When applying RCGCA to our proposed 2-layer IC framework, the number of colors N_{color}^{sub} in each sub-color pool and the number of sub-color pools N_{sub} need to be determined. In Table II, nine possible cases obtained from different combinations of N_{color}^{sub} and N_{sub} are listed. The 50% sum capacity (which is the sum capacity at CDF of 50%) obtained for each case when eight clusters are formed in each cell is plotted in Fig. 7. It can be seen clearly in Fig. 7 that the highest capacity is obtained when $N_{sub} = N_{color}^{sub} = 2$.

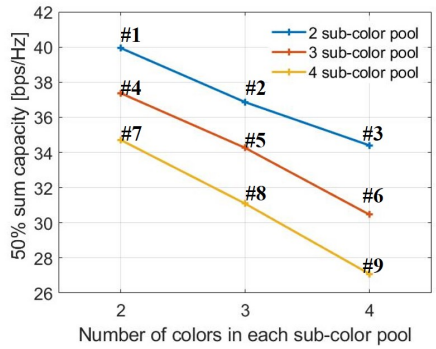

Fig. 7. 50% sum capacity comparison for different settings of N_{sub} and N_{color}^{sub}

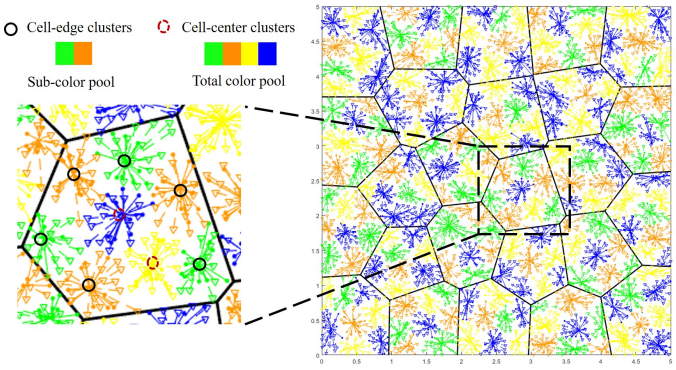

Fig. 8. An example of coloring result for 2-layer IC framework based on RCGCA

Accordingly, the restricted maximum number of colors M should be set to $M = N_{sub} = 2$ for the 1st layer IC, and $M = N_{color}^{total} = N_{color}^{sub} \times N_{sub} = 4$ for the 2nd layer IC.

As explained in Section IV, there is a tradeoff between interference mitigation and capacity improvement. Although increasing the total number of colors N_{color}^{total} can achieve better interference mitigation, the transmission bandwidth is made narrower, and therefore, increasing N_{color}^{total} does not necessarily result in a higher capacity. To restrict the value of N_{color}^{total}, N_{sub} needs to be restricted first in the 1st layer IC. Therefore, $N_{sub} = 2$ is considered to be a good compromise between interference mitigation and bandwidth reduction. In the 2nd layer IC, because the cell-edge clusters are along the cell boundary, most of the intracell interference among them can be mitigated by assigning two colors in the sub-color pool in turn. Therefore, $N_{color}^{sub} = 2$ can be used for cell-edge coloring. For coloring the inner-cell clusters, the total available color pool $N_{color}^{total} = 4$ can be used. The coloring result with eight clusters is illustrated in Fig. 8.

2) **User capacity comparison**

To verify the effectiveness of our proposed 2-layer IC framework based on RCGCA, we compare it with the well-known dynamic FFR scheme, 1-color's case (no IC), FC framework, and FD framework. We compare the capacity of cell-edge users and inner-cell users

TABLE I
SIMULATION SETTINGS

Total number of DAs in service area, N_A^{total}	3200
Total number of users in service area, N_U^{total}	2400
Number of clusters in each cell, N_C^{cell}	5-11
Pathloss exponent,α	3.5
Shadowing standard deviation, σ[dB]	8
Fading type	Rayleigh fading
Number of user location patterns	100
Number of shadowing generation per user location pattern	10
Number of fading generation per shadowing generation	10

TABLE II
PARAMETER SETTING

N_{color}^{sub} \ N_{sub}	2	3	4
2	case #1	case #2	case #3
3	case #4	case #5	case #6
4	case #7	case #8	case #9

separately when eight clusters are formed in each cell. From the results shown in Fig. 9, it can be clearly seen that the dynamic FFR, which aims at improving the performance of cell-edge users, can significantly improve the capacity of cell-edge users. However, as a common result, the improvement is at the expense of the capacity of the inner-cell users. Whereas our proposed RCGCA, fair performance can be observed no matter it is applied to FD, FC, or 2-layer IC frameworks. For cell-edge users, our proposed 2-layer IC framework based on RCGCA can achieve 47% of the FC framework when CDF = 10%, while the FD framework can achieve only 36% of the FC framework. Therefore, compared with the FD framework, our proposed 2-layer framework based on RCGCA can achieve a performance closer to the FC framework.

3) **Sum capacity comparison**

In Fig. 10, the 50% sum capacity is plotted as a function of the number of clusters per cell (varied from 5 to 11). Compared with Fig. 3 in Section II, the performance of our proposed 2-layer IC framework based on RCGCA is in between that of the FC and FD frameworks. The capacity achieved by our proposed 2-layer IC framework based on RCGCA approaches an average of 89% of the FC framework capacity, while the FD framework can only achieve an average of 84% of the FC framework capacity. In addition, compared with the 1-color's case, our proposed 2-layer IC framework based on RCGCA increases the 50% sum capacity by approximately 37% on average, while the capacity increase by the dynamic FFR is only 2%.

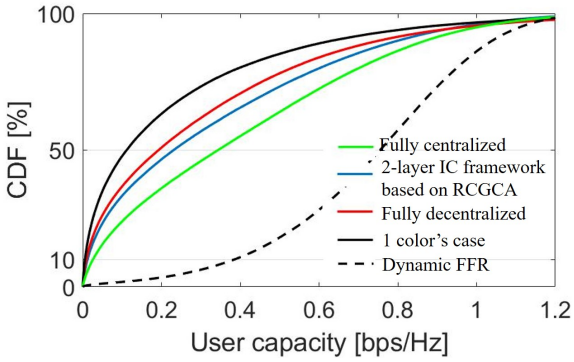

(a) Cell-edge users

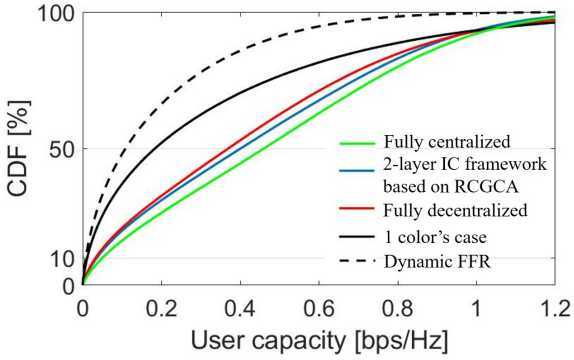

(b) Inner-cell users

Fig. 9. User capacity comparison when $N_C^{cell} = 8$

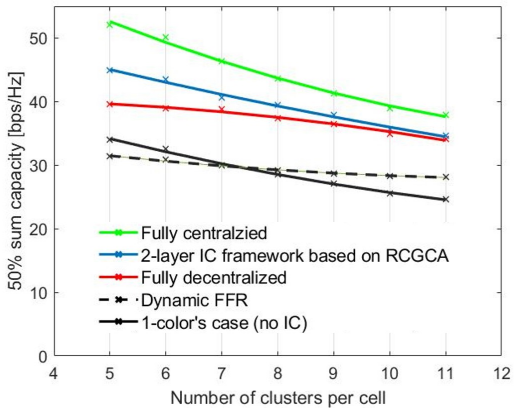

Fig. 10. Sum capacity comparison

VII. CONCLUSION

In this study, we firstly proposed a 2-layer interference coordination (IC) framework to be applied under the O-RAN architecture to jointly mitigate the intercell and intracell interferences in cellular systems with cluster-wise distributed MU-MIMO. In the 1st layer, the intercell IC is performed in a centralized manner by non-real-time RIC and then, under the conditions of the results of the 1st layer, intracell IC is performed by each near-real-time RICs in a decentralized manner in the 2nd layer.

We then proposed a restricted conditional graph coloring algorithm (RCGCA) that can be applied to the 2-layer

IC framework. The proposed RCGCA is designed to be applied on a partial pre-colored graph, which enables that when RCGCA is applied to the 2-layer IC framework, the requirement that the 2^{nd} layer coloring must be done under the condition of the pre-coloring results in the 1^{st} layer can be satisfied. Additionally, the RCGCA is designed to restrict the total number of colors, which enables RCGCA to tradeoff between improving the capacity due to interference mitigation and degrading the capacity due to bandwidth partition, thereby maximizing the link capacity.

We confirmed using computer simulations that the proposed 2-layer IC framework based on RCGCA significantly improves the capacity compared with the dynamic FFR scheme. In addition, the proposed 2-layer IC framework based on RCGCA is able to obtain results similar to the fully centralized framework with the computational complexity close to that of the fully decentralized framework.

In the future, we think the performance comparison of our proposed 2-layer IC framework based on RCGCA in both co-located MU-MIMO system and distributed MU-MIMO system will be an interesting future work.

REFERENCES

[1] Cisco, "Cisco visual networking index: Global mobile data traffic forecast update, 2017-2022," White paper, February, 2019. Available: http://media.mediapost.com/uploads/CiscoForecast.pdf

[2] X. Ge, S. Tu, G. Mao, C. -X. Wang and T. Han, "5G Ultra-Dense Cellular Networks," *IEEE Wireless Communications*, vol. 23, no. 1, pp. 72-79, February 2016, doi: 10.1109/MWC.2016.7422408

[3] J. Chen, X. Ge and Q. Ni, "Coverage and Handoff Analysis of 5G Fractal Small Cell Networks," *IEEE Transactions on Wireless Communications* , vol. 18, no. 2, pp. 1263-1276, Feb. 2019, doi: 10.1109/TWC.2018.2890662.

[4] D. Gesbert, M. Kountouris, R. W. Heath, C. Chae and T. Salzer, "Shifting the MIMO Paradigm," *IEEE Signal Processing Magazine* , vol. 24, no. 5, pp. 36-46, Sept. 2007, doi: 10.1109/MSP.2007.904815.

[5] E. G. Larsson, O. Edfors, F. Tufvesson and T. L. Marzetta, "Massive MIMO for next generation wireless systems," *IEEE Communications Magazine* , vol. 52, no. 2, pp. 186-195, February 2014, doi: 10.1109/MCOM.2014.6736761.

[6] M. Shafi, A. F. Molisch, P. J. Smith, and T. Haustein, "5G: A Tutorial Overview of Standards, Trials, Challenges, Deployment, and Practice," *IEEE Journal on Selected Areas in Communications* , vol. 35, no. 6, pp.

[7] J. Joung, Y. K. Chia and S. Sun,"Energy-Efficient, Large-Scale Distributed-Antenna System (L-DAS) for Multiple Users," *IEEE Journal of Selected Topics in Signal Processing*, vol. 8, no. 5, pp. 954-965, Oct. 2014.

[8] S. Xia, C. Ge, Q. Chen and F. Adachi, "A Study on User-antenna Cluster Formation for Cluster-wise MU-MIMO," *2020 23rd International Symposium on Wireless Personal Multimedia Communications (WPMC)*, 2020, pp. 1-6, doi: 10.1109/WPMC50192.2020.9309519.

[9] D. Gesbert, S. Hanly, H. Huang, S. Shamai Shitz, O. Simeone and W. Yu,"Multi-Cell MIMO Cooperative Networks: A New Look at Interference," *IEEE Journal on Selected Areas in Communications*, vol. 28, no. 9, pp. 1380-1408, Dec. 2010.

[10] J. Ma, S. Zhang, H. Li, N. Zhao and V. C. M. Leung, "Interference-Alignment and Soft-Space-Reuse Based Cooperative Transmission for Multi-cell Massive MIMO Networks," *IEEE Transactions on Wireless Communications* , vol. 17, no. 3, pp. 1907-1922, March 2018, doi: 10.1109/TWC.2017.2786722.

[11] X. Li, C. Li, S. Jin and X. Gao, "Interference Coordination for 3-D Beamforming-Based HetNet Exploiting Statistical Channel-State Information," *IEEE Transactions on Wireless Communications* , vol. 17, no. 10, pp. 6887-6900, Oct. 2018, doi: 10.1109/TWC.2018.2864976.

[12] H. Zhang, K. Yang and S. Zhang, "Resource Allocation Based on Interference Alignment With Clustering for Data Stream Maximization in Dense Small Cell Networks," *IEEE Access* , vol. 7, pp. 161831-161848, 2019, doi: 10.1109/ACCESS.2019.2951999.

[13] L. Chen, H. Xia, C. Feng and S. Wu, "Clustering-based co-tier interference coordination in dense small cell networks," *2015 IEEE 26th Annual International Symposium on Personal, Indoor, and Mobile Radio Communications (PIMRC)*, 2015, pp. 1878-1882, doi: 10.1109/PIMRC.2015.7343605.

[14] D. Qu, Y. Zhou, L. Tian and J. Shi, "User-Centric QoS-Aware Interference Coordination for Ultra Dense Cellular Networks," *2016 IEEE Global Communications Conference (GLOBECOM)*, 2016, pp. 1-6, doi: 10.1109/GLOCOM.2016.7842368.

[15] J. Mu, Y. Wei, H. Ma and Y. Li, "Spectrum Allocation Scheme for Intelligent Partition Based on Machine Learning for Inter-WBAN Interference," *IEEE Wireless Communications* , vol. 27, no. 5, pp. 32-37, October 2020, doi: 10.1109/MWC.001.1900551.

[16] B. Wang, Y. Sun, N. Zhao and G. Gui, "Learn to Coloring: Fast Response to Perturbation in UAV-Assisted Disaster Relief Networks," *IEEE Transactions on Vehicular Technology* , vol. 69, no. 3, pp. 3505-3509, March 2020, doi: 10.1109/TVT.2020.2967124.

[17] Ericsson, "R1-050764: Inter-cell interference handling for E-UTRA," 3GPP TSG RAN WG1 Meeting #42, Aug. 2005.

[18] 3GPP TSG RAN WG1, "Soft frequency reuse scheme for UTRAN LTE," R1-050507, Athens, Greece, May 2005.

[19] M. Qian, W. Hardjawana, Y. Li, B. Vucetic, X. Yang and J. Shi, "Adaptive Soft Frequency Reuse Scheme for Wireless Cellular Networks," *IEEE Transactions on Vehicular Technology* , vol. 64, no. 1, pp. 118-131, Jan. 2015, doi: 10.1109/TVT.2014.2321187.

[20] L. Yang, T. J. Lim, J. Zhao and M. Motani, "Modeling and Analysis of HetNets With Interference Management Using Poisson Cluster Process," *IEEE Transactions on Vehicular Technology* , vol. 70, no. 11, pp. 12039-12054, Nov. 2021, doi: 10.1109/TVT.2021.3114739.

[21] L. Eslami, G. Mirjalily and T. N. Davidson, "Spectrum-Efficient QoS-Aware Resource Assignment for FFR-Based D2D-Enabled Heterogeneous Networks," *IEEE Access* , vol. 8, pp. 218186-218198, 2020, doi: 10.1109/ACCESS.2020.3041770.

[22] A. D. Firouzabadi, A. M. Rabiei and M. Vehkaperä, "Fractional Frequency Reuse in Random Hybrid FD/HD Small Cell Networks With Fractional Power Control," *IEEE Transactions on Wireless Communications* , vol. 20, no. 10, pp. 6691-6705, Oct. 2021, doi: 10.1109/TWC.2021.3075987.

[23] M. Song, H. Shan, H. H. Yang and T. Q. S. Quek, "Joint Optimization of Fractional Frequency Reuse and Cell Clustering for Dynamic TDD Small Cell Networks," *IEEE Transactions on Wireless Communications* , vol. 21, no. 1, pp. 398-412, Jan. 2022, doi: 10.1109/TWC.2021.3096383.

[24] M. Nafees, J. Thompson and M. Safari, "Multi-Tier Variable Height UAV Networks: User Coverage and Throughput Optimization," *IEEE Access* , vol. 9, pp. 119684-119699, 2021, doi: 10.1109/ACCESS.2021.3107674.

[25] X. Li, Z. Liu, N. Qin and S. Jin, "FFR Based Joint 3D Beamforming Interference Coordination for Multi-Cell FD-MIMO Downlink Transmission Systems," *IEEE Transactions on Vehicular Technology* , vol. 69, no. 3, pp. 3105-3118, March 2020, doi: 10.1109/TVT.2020.2968095.

[26] T. Saito and F. Adachi, "De-Centralized Adaptive 2-Step Inter-cell Interference Coordination in Distributed MIMO," *2018 24th Asia-Pacific Conference on Communications (APCC)*, 2018, pp. 224-228, doi: 10.1109/APCC.2018.8633471.

[27] O-RAN Alliance, "O-RAN Minimum Viable Plan and Acceleration towards Commercialization", O-RAN White Paper, June 2021

[28] W. Jiang, B. Han, M. A. Habibi and H. D. Schotten, "The Road Towards 6G: A Comprehensive Survey," *IEEE Open Journal of the Communications Society* , vol. 2, pp. 334-366, 2021, doi: 10.1109/OJCOMS.2021.3057679.

[29] A. Garcia-Saavedra and X. Costa-Pérez, "O-RAN: Disrupting the Virtualized RAN Ecosystem," *IEEE Communications Standards Magazine* , vol. 5, no. 4, pp. 96-103, December 2021, doi: 10.1109/MCOMSTD.101.2000014.

[30] S. K. Singh, R. Singh and B. Kumbhani, "The Evolution of Radio Access Network Towards Open-RAN: Challenges and Opportunities," *2020 IEEE Wireless Communications and Networking Conference Workshops (WCNCW)*, 2020, pp. 1-6, doi: 10.1109/WCNCW48565.2020.9124820.

[31] Q. H. Duong, I. Tamim, B. Jaumard and A. Shami, "A Column Generation Algorithm for Dedicated-Protection O-RAN VNF Deployment," *2022 International Wireless Communications and Mobile Computing (IWCMC)*, 2022, pp. 1206-1211, doi: 10.1109/IWCMC55113.2022.9825080.

[32] F. Mungari, "An RL Approach for Radio Resource Management in the O-RAN Architecture," *2021 18th Annual IEEE International Conference on Sensing*, Communication, and Networking (SECON), 2021, pp. 1-2, doi: 10.1109/SECON52354.2021.9491579.

[33] H. Lee, J. Cha, D. Kwon, M. Jeong and I. Park, "Hosting AI/ML Workflows on O-RAN RIC Platform," *2020 IEEE Globecom Workshops* (GC Wkshps, 2020, pp. 1-6, doi: 10.1109/GCWkshps50303.2020.9367572.

[34] A. K. Singh and K. Khoa Nguyen, "Joint Selection of Local Trainers and Resource Allocation for Federated Learning in Open RAN Intelligent Controllers," *2022 IEEE Wireless Communications and Networking Conference (WCNC)*, 2022, pp. 1874-1879, doi: 10.1109/WCNC51071.2022.9771700.

[35] H. Kumar, V. Sapru and S. K. Jaisawal, "O-RAN based proactive ANR optimization," *2020 IEEE Globecom Workshops* (GC Wkshps, 2020, pp. 1-4, doi: 10.1109/GCWkshps50303.2020.9367582.

[36] A. S. Abdalla, P. S. Upadhyaya, V. K. Shah and V. Marojevic, "Toward Next Generation Open Radio Access Networks–What O-RAN Can and Cannot Do!," *IEEE Network (early access)*, doi: 10.1109/MNET.108.2100659.

[37] J. A. Hartigan and M. A. Wong, "Algorithm AS 136: A k-means clustering algorithm," *Journal of the Royal Statistical Society. Series C (Applied Statistics)* , vol. 28, no. 1, pp. 100–108, 1979, https://doi.org/10.2307/2346830.

[38] M. de Berg, O. Cheong, M. van Kreveld, and M. Overmars, *Computational Geometry: Algorithm and Applications*, Springer Berlin Heidelberg, Jan. 2008, doi:10.1007/978-3-540-77974-2.

[39] A S. Asratian, T M. J. Denley, R. Häggkvist, "Bipartite Graphs and their Applications," *Cambridge Tracts in Mathematics, Cambridge University Press* , 1998, doi:10.1017/CBO9780511984068.

[40] R. L. Graham and P. Hell, "On the History of the Minimum Spanning Tree Problem," *Annals of the History of Computing* , Vol. 7, No. 1, pp. 43-57, Jan.-March 1985, doi: 10.1109/MAHC.1985.10011.

[41] Y. Meng, Y. Dong, X. Liu and Y. Zhao, "An Interference-Aware Resource Allocation Scheme for Connectivity Improvement in Vehicular Networks," *IEEE Access* , vol. 6, pp. 51319-51328, 2018, doi: 10.1109/ACCESS.2018.2867745.

[42] M. K. Dholey, D. Sinha, S. Mukherjee, A. K. Das and S. K. Sahana, "A Novel Broadcast Network Design for Routing in Mobile Ad-Hoc Network," *IEEE Access* , vol. 8, pp. 188269-188283, 2020, doi: 10.1109/ACCESS.2020.3030802.

[43] V. Freschi and E. Lattanzi, "A Prim–Dijkstra Algorithm for Multihop Calibration of Networked Embedded Systems," *IEEE Internet of Things Journal* , Vol. 8, No. 14, pp. 11320-11328, 15 July, 2021, doi: 10.1109/JIOT.2021.3051270.

[44] H. Edelsbrunner, D. G. Kirkpatrick, and R. Seidel, "On the Shape of a Set of Points in the Plane," *IEEE Transaction on Information Theory* , Vol. 29, pp. 551-559, July 1983, doi: 10.1109/TIT.1983.1056714

[45] A. Pravin Renold and S. Chandrakala, "Convex-Hull-Based Boundary Detection in Unattended Wireless Sensor Networks," *IEEE Sensors Letters* , Vol. 1, pp. 2475-1472, Aug. 2017, doi: 10.1109/LSENS.2017.2731200.

[46] C. Ge, S. Xia, Q. Chen and F. Adachi, "An Improved Method in Graph Coloring Algorithm for Interference Coordination in Cluster-wise Ultra-dense RAN," *2020 International Symposium on Antennas and Propagation (ISAP)*, 2021, pp. 293-294, doi: 10.23919/ISAP47053.2021.9391334.

[47] M. Aslan and N. A. Baykan , "A Performance Comparison of Graph Coloring Algorithms", *International Journal of Intelligent Systems and Applications in Engineering* , vol. 4, no. Special Issue-1, pp. 1-7, Dec. 2016, doi:10.18201/ijisae.273053.

[48] L. Lovasz, "Three Short Proofs in Graph Theory", *Journal of Combinatorial Theory (B)* vol. 19, no. 3, pp. 269-271, December 1975, https://doi.org/10.1016/0095-8956(75)90089-1.

[49] A. H. Gebrenedhin, "Parallel Graph Coloring", Thesis, Dept. Informatics, University of Bergen, Norway, 1999. Available: https://eecs.wsu.edu/ assefaw/publications/msthesis.pdf

[50] R. M. R. Lewis, A Guide to Graph Colouring: Algorithm and Applications, *Springer International Publishing*, 2016, doi: 10.1007/978-3-319-25730-3

[51] Q. Du and T. Wong, "Numerical Studies of MacQueen's k-Means Algorithm for Computing the Centroidal Voronoi Tessellations," *Computer Mathematics with Applications* , Vol. 44, pp. 511-523, Aug. 2002, doi: 10.1016/S0898-1221(02)00165-7

[52] Q. H. Spencer, A. L. Swindlehurst, and M. Haardt, "Zero-Forcing Methods for Downlink Spatial Multiplexing in Multiuser MIMO Channels," *IEEE Transactions on Signal Processing* , Vol. 52, pp. 461-471, Jan. 2004, doi: 10.1109/TSP.2003.821107.

[53] C. Ge, S. Xia, Q. Chen and F. Adachi, "2-step Graph Coloring Algorithm for Cluster-wise Distributed MU-MIMO in Ultra-dense RAN," *2020 23rd International Symposium on Wireless Personal Multimedia Communications (WPMC)*, 2020, pp. 1-6, doi: 10.1109/WPMC50192.2020.9309477.

Chang Ge (Student Member, IEEE) received the B.E. and M.S. degrees from Northwestern Polytechnical University, Xi'an, China, in 2014 and 2017, respectively. She is now currently working toward the Ph.D. degree with the School of Engineering, Tohoku University, Sendai, Japan. Her research focuses on the large-scale distributed-antenna system, massive MIMO, interference coordination in ultra-dense network, and the application of deep learning in wireless communications.

Sijie Xia (Student Member, IEEE) received the B.E. degree from Zhengzhou University, Zhengzhou, China in 2018, and M.E. degree from Tohoku University, Sendai, Japan in 2021. He is now pursuing the Ph. D. degree at the Tohoku University. His research interests are signal processing, resource allocation, and system deployment for ultra-dense distributed antenna system.

Qiang Chen (Senior Member, IEEE) received the B.E. degree from Xidian University, Xi'an, China, in 1986, the M.E. and D.E. degrees from Tohoku University, Sendai, Japan, in 1991 and 1994, respectively. He is currently Chair Professor of Electromagnetic Engineering Laboratory with the Department of Communications Engineering, Faculty of Engineering, Tohoku University. His primary research interests include antennas, microwave and millimeter wave, electromagnetic measurement and computational electromagnetics.

Dr. Chen received the Best Paper Award and Zen-ichi Kiyasu Award in 2009 from the Institute of Electronics, Information and Communication Engineers (IEICE). He served as the Chair of IEICE Technical Committee on Photonics-applied Electromagnetic Measurement from 2012 to 2014, the Chair of IEICE Technical Committee on Wireless Power Transfer from 2016 to 2018, the Chair of IEEE Antennas and Propagation Society Tokyo Chapter from 2017 to 2018. He is now the Chair of IEICE Technical Committee on Antennas and Propagation. IEICE Fellow.

Fumiyuki Adachi (IEEE M'79-SM'90-F'02-LF'16) received the B.S. and Dr. Eng. degrees in electrical engineering from Tohoku University, Sendai, Japan, in 1973 and 1984, respectively. In April 1973, he joined the Electrical Communications Laboratories of NTT and conducted research on digital cellular mobile communications. From July 1992 to December 1999, he was with NTT DOCOMO, where he led a research group on wideband/broadband wireless access for 3G and beyond. Since January 2000, he has been with Tohoku University, Sendai, Japan. Since January 2000, he has been with Tohoku University. Currently, he is leading a resilient wireless communication research group at the International Research Institute of Disaster Science, Tohoku University, towards the development of beyond 5G systems. His research interests are in the area of wireless signal processing and networking, including multi-access, equalization, antenna diversity, adaptive transmission, channel coding, radio resource management, etc.

Dr. Adachi is a recipient of IEEE VTS Avant Garde Award 2000, IEICE Achievement Award 2002, Thomson Scientific Research Front Award 2004, Prime Minister Invention Award 2010, CC Prize 2014, IEEE VTS Stuart Meyer Memorial Award 2017, IEEE ComSoc RCC Technical Recognition Award 2017, APCC2019 Best Paper Award, etc.